RSC Advances

ROYAL SOCIETY OF CHEMISTRY

www.rsc.org/advances

Cite this: DOI: 10.1039/c0xx00000x

www.rsc.org/xxxxxx

ARTICLE TYPE

Dopamine Functionalized Polymeric Nanoparticle for Targeted Drug Delivery†

Pradip Das and Nikhil R. Jana*

Received (in XXX, XXX) Xth XXXXXXXXX 20XX, Accepted Xth XXXXXXXXX 20XX

DOI: 10.1039/b000000x

Biocompatible drug delivery nanocarrier with cellular and subcellular targeting property can greatly enhance the therapeutic effect towards various diseases. Here, we report polyaspartamide based functional polymeric nanoparticle as drug delivery carrier for targeting at cellular and subcellular length scale. The polymeric nanoparticle has polyaspartamide backbone with both octadecyl and dopamine functional groups and produces polymeric nanoparticle in water with the exposed dopamine. This polymeric nanoparticle has good encapsulation efficiency for hydrophobic drug and offers cellular delivery of drug into dopamine receptor positive human colon adenocarcinoma cells. Using this approach three different drugs (e.g. curcumin, camptothecin and doxorubicin) are selectively delivered to human colon adenocarcinoma cells. Subcellular imaging study shows that delivered drugs retain their ability to target subcellular organelles and thus curcumin targets mitochondria and doxorubicin targets nucleus. This polymeric nanoparticle can be used as alternative drug delivery carrier for *in vitro* and *in vivo* applications.

Introduction

Variety of nanoscale carriers have been developed for efficient and targeted drug delivery. These nanocarriers are generally composed of liposome,[1] porous material,[2] nanoparticle,[3] graphene[4] and polymer micelle.[5] Surface of these carriers are functionalized for specific targeting and size of nanocarrier is appropriately designed to induce enhanced permeation retention effect.[1-7] These nanocarriers can accommodate drug, travel to target site and then release drug in required time span. Some common issues of existing nanocarriers are poor colloidal stability in biological medium,[8] high nonspecific uptake by cell/tissue,[9] cytotoxicity,[10] biodegradability[11] and poor clearance.[12] Current research focus on biocompatible and biodegradable carrier with high targeting efficiency, controlled and bioresponsive drug release option and simultaneous delivery of multiple drugs.[13]

Biopolymer based nanocarriers are most attractive drugs delivery carrier because of high biocompatibility, low side effects to normal cells and biodegradability.[14-19] Commonly used biopolymers for such purpose include chitosan,[14] polylactic acid,[15] polylactic-polyglycolic acid,[16] polyethylene glycol functionalized polylactic acid,[17] functional dextran[18] and functional polyaspartic acid.[19] These biopolymers are transformed into nanoparticle or polymer micelle and appropriately functionalized for targeted delivery. Among them highly hydrophilic biopolymers such as dextran, chitosan and polyaspartic acid need extensive structural modification for transformation into nanoparticle or micelle.[14,18,19] Polyaspartic acid is one of the important poly(amino acid) that can be transformed into different functional polymers suitable for drug delivery carriers, coating material for nanoparticle and in other applications.[19-25] Polyaspartic acid can be easily synthesized from L-aspartic acid via polysuccinimide intermediate and the succinimide ring can be opened by reacting with different molecules.[21] This approach has been used in deriving variety of functional polyaspartic acids. For example, dodecyl grafted polyaspartamide has been used for coating of hydrophobic iron oxide nanoparticle,[20] cysteine functionalized polyaspartic acid has been used as coating for gold nanoparticle and quantum dot,[21] amphiphilic poly(L-aspartic acid-co-lactic acid) based polymer nanoparticles has been used as drug deliver carrier,[22] 1-(3-aminopropyl) imidazole functionalized polyaspartamide derivatives based micelle has been used for pH sensitive drug delivery,[23] polyaspartic acid based polymers has been used as vesicle component for intracellular delivery of photosensitizer,[24] poly(2-hydroxyethyl-co-octadecyl aspartamide) based polymersome with NIR fluorescence property has been synthesized for *in vivo* bioimaging application.[25] In these works polyaspartic acid generally function as hydrophilic component and linked with hydrophobic molecule in deriving polymeric nanoparticle. In addition polymeric nanoparticle is appropriately functionalized for different application. Herein, we report a new polyaspartamide polymer which is functionalized with both octadecyl and dopamine groups. In aqueous phase this polymer self-assembles into nanoparticle of 100-300 nm size with the surface exposed dopamine groups. This polymeric nanoparticle can encapsulate different hydrophobic drugs and selectively deliver them to the cells having overexpressed dopamine receptors.

Recently, dopamine functionalized small molecule and polymer

have been used for capping of metal oxide nanoparticle,[26-28] and dopamine based polymer has been reported as coating polymer for nanoparticle.[29] Dopamine is a catecholamine and acts as hormone and neurotransmitter.[30] It plays important role in central nervous system of brain through five subtypes of dopamine receptors.[30] Thus dopamine functionalized nanocarriers have great advantage in the treatment of various neurodegenerative disorders.[31] In addition dopamine receptors are over expressed on certain cancer cells[32] and thus dopamine functionalized quantum dot has been used for specific targeting of cancer cells that have dopamine receptors.[33,34] Here we show that dopamine functionalized polymeric nanoparticle can selectively deliver anticancer drugs curcumin, camptothecin and doxorubicin to human colon adenocarcinoma cells and expected to be an alternative drug delivery carrier for *in vitro* and *in vivo* applications.

Experimental Section

Materials

L-aspartic acid, octadecylamine (ODA), triethylamine, dopamine hydrochloride (D), dimethyl sulfoxide-d_6, curcumin, camptothecin and doxorubicin hydrochloride were purchased from Sigma-Aldrich. Phosphoric acid (88 %, H_3PO_4) was purchased from Merck. Mesitylene and dry dimethylformamide were purchased from Spectrochem. Dulbecco's modified eagle medium (DMEM) and penicillin/streptomycin were purchased from Sigma-Aldrich. Fetal bovine serum (FBS) was purchased from Life technologies. 3-(4,5-Dimethylthiazol-2-yl)-2,5-diphenyltetrazolium bromide (MTT) was purchased from HiMedia. Lysotracker red and mitotracker red were purchased from Invitrogen.

Synthesis of polysuccinimide (PSI)

Polysuccinimide was synthesized by acid catalyzed polycondensation of L-aspartic acid following reported method with some modifications.[35] Briefly, 3 g of L-aspartic acid was suspended in 12 mL mesitylene, mixed with 165 µL phosphoric acid (88 %) and heated at 150 °C for 4.5 hrs under inert atmosphere. After cooling, white residue was dissolved in dimethylformamide and then excess water was added to precipitate the polysuccinimide. The precipitate was washed with water to remove phosphoric acid and dimethylformamide and then washed with methanol several times. Finally, solid polysuccinimide was dried in vacuum.

Synthesis of octadecylamine and dopamine functionalized polysuccinimide (ODA-PSI-D)

250 mg polysuccinimide was dissolved in 20 mL dry dimethylformamide, mixed with 135 mg (or 405 mg) octadecylamine and heated at 70 °C for 24 hrs under inert atmosphere. (Table 1) The solution was cooled to room temperature and mixed with 76 mg (or 208 mg) dopamine hydrochloride and 56 µL (or 168 µL) triethylamine. The mixture was further heated at 70 °C under inert atmosphere for 24 hrs. The resultant ODA-PSI-D was precipitated by adding excess methanol-diethyl ether mixture (1:1 volume ratio). The precipitate was washed with methanol-diethyl ether mixture for several times and dried under vacuum.

Table 1. Reaction conditions used to prepare three different polysuccinimide (ODA-PSI-D) for varying the degree of substitution of octadecyl and dopamine.

Sample	PSI	ODA	Dopamine
ODA-PSI-D (P1)	250 mg	135 mg	76 mg
ODA-PSI-D (P2)	250 mg	405 mg	76 mg
ODA-PSI-D (P3)	250 mg	135 mg	228 mg

Determination of critical aggregation concentration (CAC)

The critical aggregation concentration of ODA-PSI-D was determined using nile red as fluorescent probe.[36] Typically, 50 µL acetone solution of nile red (1×10^{-6} M) was added to several of 5 mL vials and allowed to stand for overnight. Once acetone is evaporated, 2 mL ODA-PSI-D solution was added to each of the nile red containing vials. ODA-PSI-D solution was prepared in 0.1-0.3 % DMF-water with the concentration range of 0.001-0.1 mg/mL by diluting the stock solution of polymer prepared in 10 % DMF-water mixture and having 2.5 mg/mL concentration. Then solutions were allowed to equilibrate at room temperature for 24 hrs. Next, fluorescence of nile red was measured under 485 nm excitation and fluorescence intensity of nile red at 612 nm was plotted against concentration of ODA-PSI-D. The critical aggregation concentration of ODA-PSI-D was determined from inflection point of the plot.

Synthesis of drug encapsulated polymeric nanoparticle

Dimethylformamide solution of curcumin or camptothecin or doxorubicin was prepared with a concentration of 1 mg/mL. Next, 150 µL drug solution was mixed with 0.5 mL dimethylformamide solution of 10 mg ODA-PSI-D. This mixture was then drop wise added to the 5 mL water under vigorously stirring condition and stirring was continued for 4 hrs. The excess organic solvent and free drug were then removed via dialysis of the whole mixture against distilled water using dialysis membrane (MWCO ~ 12000-14000 Da).

The amount of drug encapsulated into ODA-PSI-D polymeric nanoparticle was determined using the absorbance of drug at the corresponding wavelength (425 nm, 366 nm and 490 nm for curcumin, camptothecin and doxorubicin, respectively). The encapsulation efficiency of drug into ODA-PSI-D polymeric nanoparticle was determined by the following equation: Encapsulation efficiency (%) = (Amount of drug encapsulated/Amount of drug used) × 100.

In vitro drug release study

One mL of drug encapsulated ODA-PSI-D polymeric nanoparticle solution was loaded inside dialysis tube (MWCO ~ 12000-14000 Da) and dialysis was performed against 100 mL PBS buffer solution of pH 7.4 under stirring condition. At certain time intervals, 200 µL of phosphate buffer solutions was collected and appropriately diluted with fresh buffer solution. Fluorescence of the solution was recorded at 425 nm for camptothecin (excitation 370 nm) and 600 nm for doxorubicin (excitation 490 nm).

Cellular uptake study

The dopamine receptor positive human colon adenocarcinoma

HT-29 cells and dopamine receptors negative normal mouse embryonic fibroblasts 3T3-L1 cells were cultured in Dulbecco's modified eagle medium (DMEM) supplemented with 10 % fetal bovine serum (FBS) and 1 % penicillin/streptomycin at 37 °C and 5 % CO_2. For cellular uptake studies, the cells were seeded overnight into 24-well tissue culture plates in 500 µL supplemented DMEM medium. Then cells were treated with drug encapsulated polymeric nanoparticle with the 1.65 µg/mL final concentration of the respective drug and incubated for different times (i.e., 2, 4, 8 and 12 hrs). After incubation, the cells were washed with PBS buffer and 500 µL supplemented DMEM medium was added to each well. Then live cells were imaged under fluorescence microscope. Quantification of cellular uptake of drug was performed by flow cytometry study. For flow cytometry study, cells were seeded into 24-well plates at high density and cultured in 500 µL supplemented DMEM medium at 37 °C and 5 % CO_2 for overnight. After that, drug encapsulated polymeric nanoparticle was added with final drug concentration of 1.65 µg/mL and incubated for 4 hrs. In control experiment similar study was performed in presence of 50 µL dopamine solution (10 mM). Then the cells were trypsinized after washing with PBS buffer solution and collected by centrifuge. Collected cells were washed with PBS buffer solution. Finally, the cells were dispersed in PBS buffer solution and examined by flow cytometry for quantitative uptake study. The cell without any labeling was used as negative control.

In vitro cytotoxicity study

The cytotoxicity of polymeric nanoparticle, free drug and drug encapsulated polymeric nanoparticle against HT-29 and 3T3-L1 cells were evaluated by conventional MTT assay. In brief, the cells were seeded at high density into 24-well tissue culture plate containing 500 µL DMEM media supplemented with 10 % FBS and 1 % penicillin/streptomycin and cultured overnight at 37 °C and 5 % CO_2. After that, cells were incubated for 24 hrs with polymer micelle or free drug or drug encapsulated polymeric nanoparticle of different concentrations. Next, cells were washed with PBS buffer solution and 500 µL fresh supplemented DMEM medium was added to each well. Then, 50 µL of aqueous solution of MTT (5 mg/mL) was added and incubated for 4 hrs. The supernatant in each well was discarded and violet formazan was dissolved in 500 µL of sodium dodecyl sulfate solution in water/DMF mixture. The absorbance at 570 nm was measured using microplate reader. The cell viability was calculated by assuming 100 % cell viability for cells without any sample.

Instrumentation

UV-visible absorption and fluorescence spectral studies were carried out on Shimadzu UV-2550 UV-visible spectrophotometer and BioTek SynergyMx microplate reader, respectively. The field emission scanning electron microscopy (FESEM) analysis was performed with a Supra 40, Carl Zeiss Pvt. Ltd. instrument. The molecular weight of polymer was analyzed using gel permeation chromatography (GPC) consisting of Waters 515 HPLC pump and Waters 2414 refractive index detector equipped with HSPgelTM AQ 4.0 column (6.0 X 150 mm) and calibrated with dextran standard. The sample was injected at 0.3 mL/minute flow rate with water based mobile phase supplemented with 0.05 % sodium azide. The ^{1}H NMR (400 MHz) spectra were recorded on a Bruker DPX-400 spectrometer by using DMSO-d_6 as solvent at room temperature. FTIR spectra of the samples compressed into KBr pellets were measured on Perkin Elmer Spectrum 100 FTIR spectrometer. The hydrodynamic sizes and zeta potentials were measured using NanoZS (Malvern) instrument. Differential interference contrast and fluorescence images of live cells were performed by Olympus IX81 microscope using image-pro plus version 7.0 software. The quantitative cellular uptake of curcumin or doxorubicin encapsulated polymer micelle was performed on BD Accuri C6 Flow Cytometer.

Results and discussion

Synthesis and characterization of dopamine functionalized polysuccinimide

The chemical structure and steps for synthesis of polymeric nanoparticle is shown in Scheme 1. It consists of polysuccinimide backbone functionalized with both octadecyl and dopamine (ODA-PSI-D). The octadecyl group offers hydrophobicity to the polymer that induces nanoparticle formation and dopamine would expose to aqueous phase. Synthesis of ODA-PSI-D involves three steps. First, polysuccinimide (PSI) is synthesized by phosphoric acid catalyzed thermal polycondensation of L-aspartic acid. Next, succinimide groups of PSI are reacted with different amount octadecylamine (ODA) and dopamine (D) in two successive steps.

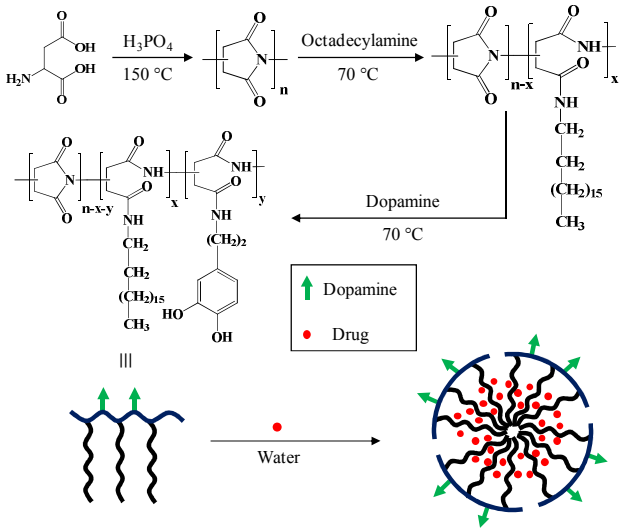

Scheme 1. Three step synthetic route of octadecylamine and dopamine functionalized polysuccinimide (ODA-PSI-D) and formation of drug encapsulated polymeric nanoparticle. First, polysuccinimide (PSI) is synthesized by phosphoric acid catalyzed polycondensation of L-aspartic acid. Next, aminolysis of succinimide groups of PSI is performed with octadecylamine (ODA) and dopamine (D) in two successive steps. Finally, dimethylformamide solution of mixture of ODA-PSI-D and drug is added to water to prepare drug encapsulated polymeric nanoparticle of ODA-PSI-D.

The molecular weight of PSI has been estimated via gel permeation chromatography after complete hydrolysis of succinimide groups under basic condition. The number average molecular weight (M_n) and weight average molecular weight (M_w) has been determined as 22500 g/mol and 30800 g/mol, respectively, with polydispersity index (PDI) of 1.37 (ESI, Fig. S1†). The ^{1}H NMR spectra of PSI and ODA-PSI-D reveal the

chemical structure of polymer (Fig. 1). The PSI shows signals at 2.7 and 3.2 ppm for methylene protons and 5.1-5.4 ppm for methine proton of succinimide unit.[35] The ^{1}H NMR spectrum of ODA-PSI-D shows the characteristic proton peaks of octadecylamine, dopamine and opened succinimide rings. The protons of methyl and methylene group of octadecyl group appear at 0.85 ppm and 1.23 ppm, respectively.[25] The characteristic proton signals of dopamine appear in the range of 6.4-6.7 ppm.[28] The appearance of proton signals at 4.5 ppm along with signal at 5.1-5.4 ppm indicates that the fraction of succinimide rings is opened during aminolysis. The degree of substitution of octadecyl and dopamine group in polysuccinimide backbone has been calculated from ^{1}H NMR spectra.[25] It has been observed that in our reaction condition the octadecyl group is varied between 15-32 mol % and dopamine is varied between 10-20 mol % (Table 2).

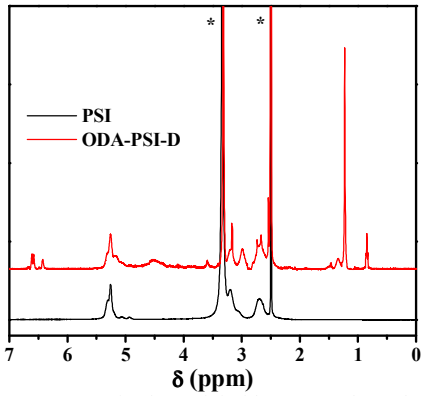

Fig. 1 ^{1}H NMR spectra of polysuccinimide (PSI) and octadecylamine and dopamine functionalized polysuccinimide (ODA-PSI-D; P1) in DMSO-d_6. Methylene protons of succinimide units shows peak at 2.7 and 3.2 ppm and methine proton peak appears in the range of 5.1-5.4 ppm. After functionalization with octadecylamine and dopamine, the characteristic peaks for long alkyl chains octadecyl groups appear at 0.85 and 1.23 ppm and the catechol protons of dopamine appears at 6.4-6.7 ppm. (* indicates solvents peaks)

Fourier transform infrared (FTIR) spectrum of PSI shows the characteristic bonding peaks of succinimide unit at 1713 cm^{-1}, 1395 cm^{-1} and 1218 cm^{-1} (ESI, Fig. S2†). These peaks are assigned to C=O stretching of cyclic imides, CH_2 vibration band and C-N stretching of cyclic imides, respectively. The PSI also shows the additional peaks of C-H stretching at around 3000 cm^{-1} and broad band at 3600-2800 cm^{-1} that indicates the presence of amide groups. In the case of ODA-PSI-D, new strong bands at 1658 cm^{-1} and 1535 cm^{-1} appear due to the two different amides. The C-H stretching band of grafted octadecylamine and dopamine appears at 2855 cm^{-1}and 2925 cm^{-1}.

Drug encapsulation by dopamine functionalized polymeric nanoparticle

We have selected three different hydrophobic drugs such as curcumin, camptothecin and doxorubicin for this study. Drug encapsulation and polymeric nanoparticle formation are involved in simple one step processes. Typically, dimethylformamide solution of mixture of ODA-PSI-D and drug are added to water under vigorous stirring condition (Scheme 1). Under such condition polymer self-assemble into nanoparticle structure keeping hydrophobic octadecyl chains together and other polar groups (carboxylate and dopamine) outside. During this processes hydrophobic drugs are encapsulated into hydrophobic domains of nanoparticle.

Table 2. Properties of three different polysuccinimide (ODA-PSI-D) synthesized with varied degree of substitution of octadecyl ($DS_{octadcyl}$) and dopamine ($DS_{dopamine}$).

Sample	$DS_{octadecyl}$ (mol %)	$DS_{dopamine}$ (mol %)	CAC (mg/mL)	Average Hydrodynamic Size (PDI)[#]
ODA-PSI-D (P1)	~ 18	~ 12	~ 0.006	180 ± 14 (0.36)
ODA-PSI-D (P2)	~ 32	~ 11	~ 0.02	350 ± 30 (0.45)
ODA-PSI-D (P3)	~ 17	~ 19	~ 0.009	300 ± 20 (0.58)

[#] polydispersity index

Nanoparticle formation and size of polymeric nanoparticle has been determined by dynamic light scattering (DLS) analysis and field emission scanning electron microscopy (FESEM). DLS study shows that hydrodynamic diameter of ODA-PSI-D increases from 2-5 nm to 100-500 nm when solvent is changed from dimethylformamide to water (Fig. 2 and Table 2 and ESI, Fig. S3†). This result indicates that ODA-PSI-D assemble into nanoparticle structure in aqueous phase. However, the size and shape of polymeric nanoparticle depends on the degree of substitution of octadecyl and dopamine groups. For example increased substitution of octadecyl group on polymer backbone increases the shape anisotropy of polymeric nanoparticle and increased substitution of octadecyl or dopamine groups increases the hydrodynamic size of nanoparticle (Fig. 2). We have selected ODA-PSI-D (P1) for our study as it produces smaller size polymeric nanoparticle of spherical morphology with average diameter of 180 nm. Stability of ODA-PSI-D (P1) based polymeric nanoparticle has been determined under different buffer solution and under longer time preservation (ESI, Fig. S4†). Hydrodynamic size of ODA-PSI-D (P1) based polymeric nanoparticle remains same at different solution pH 5-10. In addition the nanoparticle solution at physiological pH 7.4 maintained the hydrodynamic size for week. These results indicate good colloidal stability of polymeric nanoparticle and similar stability is expected under physiological environment. The surface charge of ODA-PSI-D (P1) based polymeric nanoparticle increases from -10 mV to -35 mV with the increasing solution pH from 5 to 10, which is due to increased deprotonation of surface exposed carboxylic groups (ESI, Fig. S4†).

Hydrodynamic diameter of polymeric nanoparticle has also been measured after drug encapsulation (Fig. 3 and ESI, Table S1 and Fig. S5†). Results show that average hydrodynamic size has been increased by 15-70 nm after drug encapsulation. Typical FESEM images of polymeric nanoparticle and drug encapsulated polymeric nanoparticle are shown in Fig. 2 and 3 and ESI, Fig S6†. It shows that polymeric nanoparticle of ODA-PSI-D (P1) remains spherical after drug encapsulation. Critical aggregation concentration (CAC) of three different ODA-PSI-D has been determined using nile red as fluorescent probe and it is observed that in all cases CAC values remain low (typically in the range of ~ 0.006-0.02 mg/mL) (Table 2 and ESI, Fig. S7†).[36]

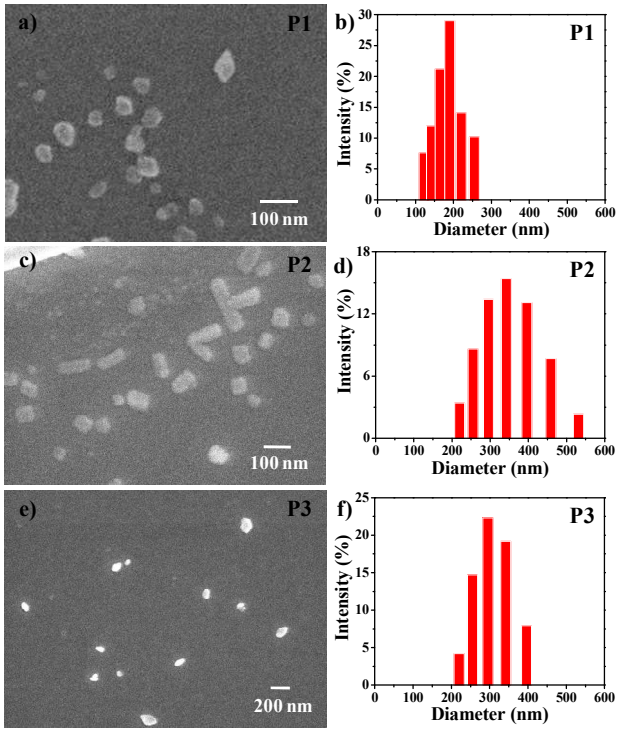

Fig. 2 Field emission scanning electron microscopy (FESEM) image and respective dynamic light scattering-based hydrodynamic size of polymeric nanoparticle made of three different ODA-PSI-D.

Presence of dopamine on the surface of polymeric nanoparticle has been tested by Fe^{3+} ion induced aggregation of polymeric nanoparticle. It is observed that curcumin encapsulated ODA-PSI-D (P1) polymeric nanoparticle aggregates immediately of adding ferric salt (ESI, Fig. S8†). Result indicates that dopamines are exposing on the surface of polymeric nanoparticle and induce their coordinative crosslinking by Fe^{3+} ions.[37]

The optical properties of drugs before and after encapsulation into polymeric nanoparticle have been investigated. The UV-visible absorption spectrum of polymeric nanoparticle shows the characteristic peak of dopamine at 280 nm with its catechol form and without any sign of polymerization (ESI, Fig. S9†).[38] Absorption and emission spectra of curcumin is measured in dimethylformamide-water mixture and compared with curcumin encapsulated into polymeric nanoparticle in water (ESI, Fig. S10†). In dimethylformamide-water curcumin shows broad absorption band at 425 nm and 355 nm of the π-π* transitions of conjugated curcumin and the feruloyl unit, respectively. However, after nanoparticle encapsulation, the band at 355 nm for feruloyl unit is disappeared but the other band at 425 nm remains intact. This suggests that feruloyl unit of curcumin that interact with water and produce 355 nm band but after encapsulation with polymeric nanoparticle such interaction is prohibited, suggesting that curcumin is localized at the hydrophobic region of the polymeric nanoparticle.[39] Similar result is also observed for fluorescence property of curcumin. Curcumin shows weak emission band at ~ 555 nm at 440 nm excitation but after nanoparticle encapsulation it show enhanced emission along with blue shifting of the emission band to ~ 515 nm. The blue-shifted emission of curcumin is due to the poor

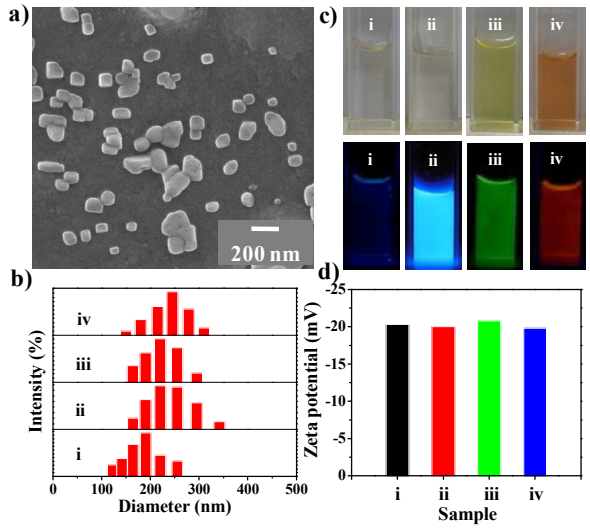

Fig. 3 a) Field emission scanning electron microscopy (FESEM) image of curcumin encapsulated ODA-PSI-D (P1) polymeric nanoparticle. b) Dynamic light scattering based hydrodynamic size of same polymeric nanoparticle before and after drug encapsulation. c) Digital image of colloidal solution of same polymeric nanoparticle before and after drug encapsulation under normal light (top row) or hand held UV light (bottom row). d) Zeta potentials of aqueous solution of same polymeric nanoparticle before and after drug encapsulation. [i) polymeric nanoparticle, ii) camptothecin encapsulated polymeric nanoparticle, (iii) curcumin encapsulated polymeric nanoparticle and (iv) doxorubicin encapsulated polymeric nanoparticle]

interaction of curcumin with water. The average lifetime of curcumin has also been increased to ~ 0.62 ns after nanoparticle encapsulation, as compared to ~ 0.22 ns in DMF-water (ESI, Fig. S10†). The emission enhancement, blue-shifting of emission band and increased life time indicate that curcumin is located into the hydrophobic environment of polymeric nanoparticle.[39]

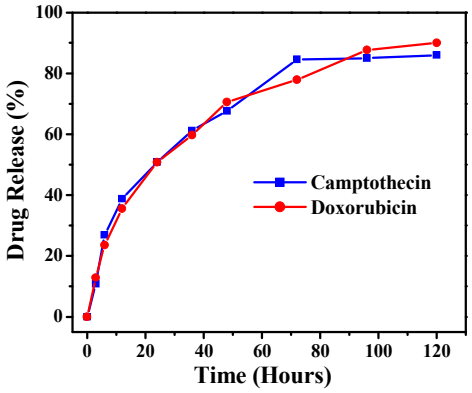

Fig. 4 *In vitro* drug release patterns of camptothecin and doxorubicin from camptothecin or doxorubicin encapsulated ODA-PSI-D (P1) polymeric nanoparticle in PBS buffer solution of pH 7.4.

Optical properties of polymeric nanoparticle encapsulated camptothecin and doxorubicin has also been studied (ESI, Fig. S11†). The camptothecin encapsulated polymeric nanoparticle shows blue emission at 425 nm (under 370 nm excitation) and doxorubicin encapsulated polymeric nanoparticle shows red emission at 600 nm (under 490 nm excitation).

The encapsulation efficiency of drugs by ODA-PSI-D (P1) based polymeric nanoparticle has been determined using UV-visible absorption of drugs (ESI, Fig. S12†). Typical encapsulation

efficiencies are in the range of 70-80 %, 60-70 % and 55-65 % for curcumin, camptothecin and doxorubicin, respectively. In contrast drug encapsulation efficiencies by ODA-PSI-D (P2) and ODA-PSI-D (P3) based polymeric nanoparticle are relatively low. This variation of encapsulation efficiency of different drugs is probably linked with the nature of drug with varied hydrophobicity. *In vitro* drug release behavior from ODA-PSI-D (P1) polymeric nanoparticle has been studied in phosphate buffer of pH 7.4 (Fig. 4). Results show that release rate of drug is moderate; typically 80-90 % release occurs in 120 hrs time. This drug release pattern indicates that drug encapsulation in polymeric nanoparticle is efficient, possibly due to the larger size of nanoparticle with larger hydrophobic core.[40]

Cellular drug delivery, intracellular drug distribution and cytotoxicity study

We have selected two different cell lines for drug delivery study. Dopamine receptors positive human colon adenocarcinoma HT-29 cells has been used to investigate the dopamine receptors induced cellular uptake and normal mouse embryonic fibroblasts 3T3-L1 cells has been used as dopamine receptors negative control cells.[32,34] The drug encapsulated polymeric nanoparticle is incubated with cells for different time interval and then washed cells are imaged under fluorescence microscope to observe the drug uptake using the fluorescence property of drugs. Results show that fluorescence of drugs is observed inside HT-29 cells indicating their internalization (Fig. 5). For example, the curcumin uptake shows green fluorescence, camptothecin uptake shows blue fluorescence and doxorubicin shows red fluorescence inside HT-29 cells. In addition it is observed that fluorescence

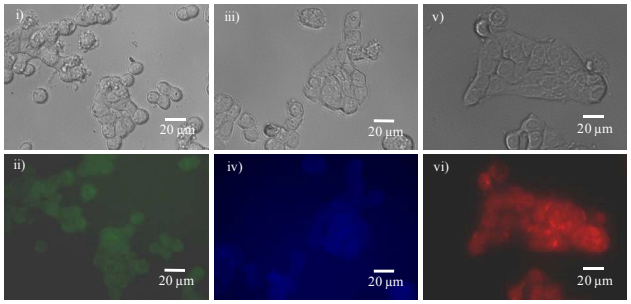

Fig. 5 Observation of uptake of curcumin (i, ii), camptothecin (iii, iv) and doxorubicin (v, vi) in HT-29 cells via fluorescence imaging. HT-29 cells are incubated with drug encapsulated ODA-PSI-D (P1) polymeric nanoparticle for 12 hrs and then washed cells are measured under microscope. Top panel shows differential interference contrast images and bottom panel shows fluorescence images obtained under UV excitation (iv), blue excitation (ii) and green excitation (vi).

inside cells increases with increasing incubation time suggesting that drug internalization increases with incubation time (ESI, Fig. S13†). In contrast, fluorescence signal has not been observed inside 3T3-L1 cells, indicating no drug uptake (ESI, Fig. S14†). If drugs are incubated without using any polymeric nanoparticle, they have insignificant uptake (except doxorubicin) by both cells (ESI, Fig. S15†). In another control experiment drug uptake by HT-29 cells has been studied in presence of excesses free dopamine in the cell culture medium (Fig. 6 and ESI, Fig. S16†). Results show the lowering of drug uptake in presence of free dopamine, suggesting that polymeric nanoparticle is internalized into HT-29 cells via dopamine receptor mediated endocytosis.

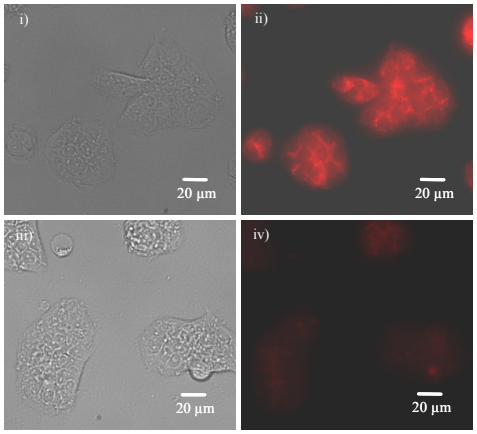

Fig. 6 Influence of free dopamine in cellular uptake of doxorubicin in HT-29 cells. HT-29 cells are incubated with doxorubicin encapsulated ODA-PSI-D (P1) polymeric nanoparticle for 4 hrs in absence (i, ii) or presence (iii, iv) of free dopamine. Next, cells are washed and imaged under differential contrast mode (i, iii) and fluorescence mode with green excitation (ii, iv).

Flow cytometry analysis has been used to quantify the uptake of drug into HT-29 and 3T3-L1 cells (Fig. 7 and ESI, Fig. S17†). Results clearly confirm the higher drug uptake by HT-29 cells as compared to 3T3-L1 cells or HT-29 cells in presence of free dopamine. Drug uptake in HT-29 cells by ODA-PSI-D (P1) and ODA-PSI-D (P3) based polymeric nanoparticle has been compared and similar uptake efficiency is observed (ESI, Fig. S18†). This result indicates that increased degree of dopamine substitution does not significantly influence the drug uptake performance.

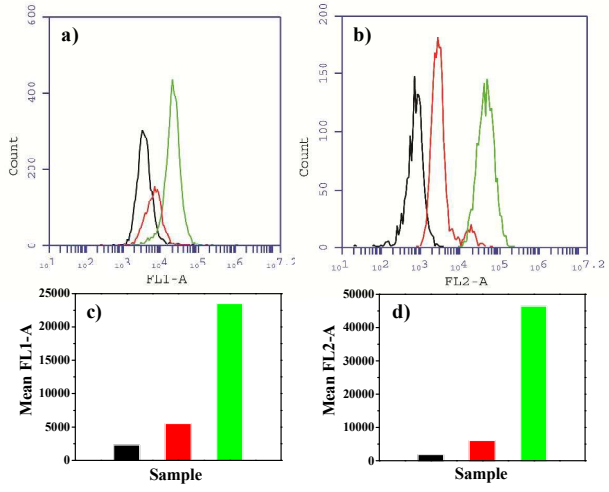

Fig. 7 Flow cytometry analysis of HT-29 cell uptake of curcumin encapsulated with ODA-PSI-D (P1) polymeric nanoparticle (a, c) and doxorubicin encapsulated with ODA-PSI-D (P1) polymeric nanoparticle (b, d) in presence of free dopamine (red line/bar) or absence of free dopamine (green line/bar). Black line/bar indicates control without polymer or drug. Cells are incubated with drug encapsulated polymeric nanoparticle for 4 hrs and washed cells are used for analysis. Mean FL1-A and FL2-A represent mean area of fluorescence signal collected by standard optical filters FL1 (533/30 nm) and FL2 (585/40 nm), respectively.

In order to understand the localization of delivered drugs inside HT-29 cells, colocalization study has been performed using different subcellular imaging probes (Fig. 8 and ESI, Fig. S19†). Lysotracker red, mitrotracker red and hoechst dye have been used as probes for lysosome, mitochondria and nucleus, respectively. Results show that fluorescence image of internalized curcumin significantly colocalizes with mitotraker red but does not colocalize with lysotraker red. This result suggests that curcumin has been specifically delivered to mitochondria. Similarly, fluorescence image of internalized doxorubicin significantly colocalizes with nuclear probe, suggesting that doxorubicin has been delivered to cell nucleus.

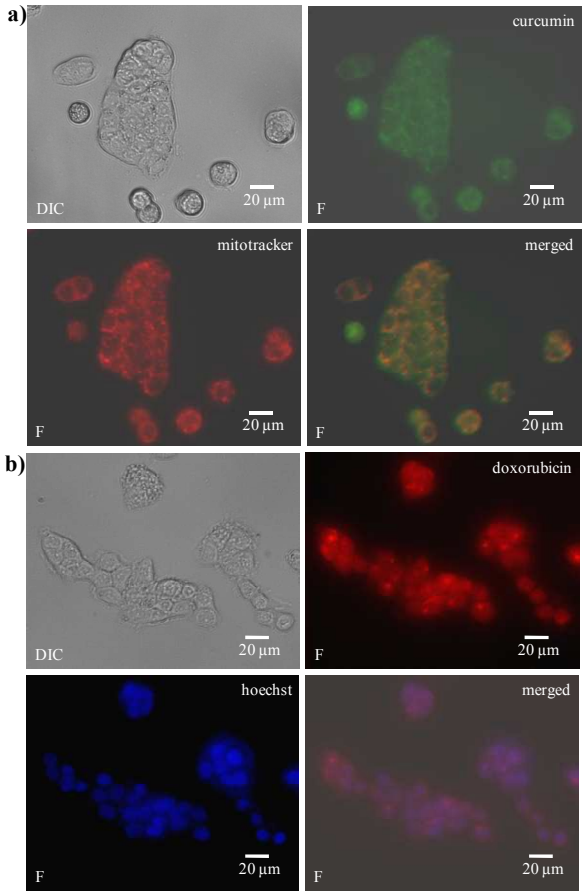

Fig. 8 Intracellular distribution of curcumin (a) and doxorubicin (b) in HT-29 cells delivered via ODA-PSI-D (P1) based polymeric nanoparticle. Cells are incubated with drug encapsulated polymeric nanoparticle for 4 hrs followed by further labeling with mitotracker red/hoechst and imaged under differential contrast mode (DIC) or fluorescence mode (F). Merged fluorescent images indicate colocalization of curcumin with mitochondria and doxorubicin with neucleus.

In vitro cytotoxicity of polymeric nanoparticle, free drug and drug encapsulated polymeric nanoparticle has been investigated using HT-29 and 3T3-L1 cells via conventional 3-(4,5-dimethylthiazol-2-yl)-2,5-diphenyltetrazolium bromide (MTT) based colorimetric assay. Typically, polymeric nanoparticle or free drug or drug encapsulated polymeric nanoparticle is incubated with cells for 24 hrs and washed cells have been used for MTT assay. Results show viability of HT-29 cells decreases significantly in presence of drug encapsulated polymeric nanoparticle and viability decreases with increasing drug concentration. In contrast viability of 3T3-L1 cells under similar condition is high in presence of drug encapsulated polymeric nanoparticle (Fig. 9). Control experiments show that toxicity of free drug (except doxorubicin) against both cells is very low because of low drug uptake (ESI, Fig. S20†). In addition it is observed that polymeric nanoparticle has no significant cytotoxicity against both HT-29 and 3T3-L1 cells even at highest tested concentration (500 µg/mL) (Fig. 9). Another control experiment shows that cytotoxicity for drug encapsulated polymeric nanoparticle to HT-29 cells decreases if free dopamine is present in cell culture medium (ESI, Fig. S21†). The observed results can be explained by enhanced drug uptake by dopamine receptors positive HT-29 cells as compared to low drug uptake by dopamine receptors negative 3T3-L1 cells. Tentative values of 50 % inhibitory concentration of free drug and drug encapsulated polymeric nanoparticle have been determined for HT-29 and 3T3-L1 cells with 24 hrs incubation. The value is > 5 µg/mL for all the free drugs against both cells. For drug encapsulated polymeric nanoparticle the value remains same for 3T3-L1 cells but decreases to 3-4 µg/mL for HT-29 cells.

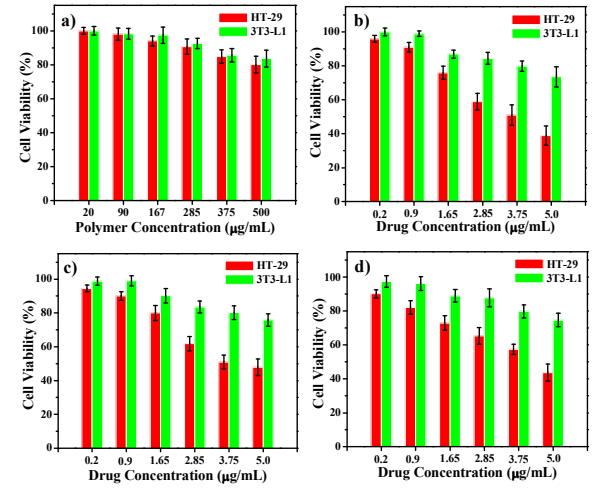

Fig. 9 *In vitro* cytotoxicity study of (a) ODA-PSI-D (P1) based polymeric nanoparticle, (b) curcumin encapsulated ODA-PSI-D (P1) polymeric nanoparticle, (c) camptothecin encapsulated ODA-PSI-D (P1) polymeric nanoparticle and (d) doxorubicin encapsulated ODA-PSI-D (P1) polymeric nanoparticle. HT-29 or 3T3-L1 cells are incubated with drug encapsulated ODA-PSI-D (P1) polymeric nanoparticle of different concentration for 24 hrs and then used for MTT based cytotoxicity study. Cell without any polymer or drug correspond to 100 % viability.

Advantage of polyaspartic acid-based nanoparticle as drug delivery carrier

Polyaspartic acid based nanocarriers have the advantage of superior biocompatibility, water solubility and biodegradability.[19,22-24] In addition polymer can be synthesized relatively easily via polysuccinimide based approach and variety of structural modification can be achieved via succinimide ring opening by amine based biomolecules. Successful functionalization of polysuccinimide with octadecylamine and dopamine indicates that functionalization with other biomolecules are also possible. In addition successful encapsulation of three drugs suggests that different types of hydrophobic and

hydrophilic drugs can be loaded into this polymeric nanoparticle. The typical size of drug encapsulated micelle of 100-300 nm is also ideal for effective *in vitro* and *in vivo* applications.[41] Commonly used drug delivery carriers that include liposomes, polymersomes, polymer nanoparticles, dendrimers and polyplexes have size in the range of 50-1000 nm.[42-44] In addition elliptical disks, cylinders and filamentous shape of delivery carrier have been tested for drug delivery.[45-47] These study show that smaller size, non-spherical shape and high colloidal stability are particularly important for targeted delivery.[41] In that respect the presented polymeric nanoparticle of 100-300 nm size and with high colloidal stability in physiological condition is very effective for targeted delivery of drugs.

Recently, particular attention has been paid on subcellular delivery of drugs as the origin of many diseases is linked at this length scale.[48] Although drugs may have subcellular targeting property, endosomal trafficking often restricts their actual effect. Thus appropriate carriers have been designed for successful subcellular targeting.[5,22,49-53] In that respect, the subcellular targeting property of drug using our polymeric nanoparticle offers significant advantage. Although the exact reason of this subcellular targeting property needs further study, the tentative reasons of this targeting may be linked with the endocytosis pathway of polymeric nanoparticle via dopamine receptors.[32-34]

Conclusion

In summary, we have synthesized dopamine functionalized polyaspartamide based polymeric nanoparticle with hydrodynamic size 100-300 nm. The polymeric nanoparticle has the ability to encapsulate the hydrophobic drugs (e.g. curcumin, camptothecin and doxorubicin) and deliver drugs to the cells having dopamine receptors. Subcellular imaging study shows that delivered drugs retain their subcellular targeting property. The polymeric nanoparticle has high colloidal stability, low nonspecific binding with cells and low cytotoxicity. Proposed synthetic strategy can be applied for preparation of other functional polyaspartamide nanoparticle and can be used as alternative drug delivery carrier for treatment of different diseases.

Acknowledgements

The authors acknowledge CSIR and DST, government of India for financial assistance. P. Das acknowledges CSIR, India for research fellowships.

Notes and references

Centre for Advanced Materials, Indian Association for the Cultivation of Science, Jadavpur, Kolkata-700032, India. E-mail: camnrj@iacs.res.in Fax:+ 91-33-24732805; Tel: + 91-33-24734971.

†Electronic Supplementary Information (ESI) available: Characterization of polymer, optical properties of polymeric nanoparticle and drug encapsulated polymeric nanoparticle, study of cellular uptake and intracellular distribution of free drugs and polymeric nanoparticle encapsulated drug. See DOI: 10.1039/b000000x/

1 A. Sharma and U. S. Sharma, *Int. J. Pharm.*, 1997, **154**, 123-140.
2 M. Vallet-Regi, F. Balas and D. Arcos, *Angew. Chem., Int. Ed.*, 2007, **46**, 7548-7558.
3 C. K. Kim, P. Ghosh, C. Pagliuca, Z.-J. Zhu, S. Menichetti and V. M. Rotello, *J. Am. Chem. Soc.*, 2009, **131**, 1360-1361.
4 A. R. Maity, A. Chakraborty, A. Mondal and N. R. Jana, *Nanoscale*, 2014, **6**, 2752-2758.
5 V. P. Torchilin, *Pharm. Res*., 2007, **24**, 1-16.
6 J. Sudimack and R. J. Lee, *Adv. Drug Delivery Rev.*, 2000, **41**, 147-162.
7 H. Koo, M. S. Huh, I.-C. Sun, S. H. Yuk, K. Choi, K. Kim and I. C. Kwon, *Acc. Chem. Res.*, 2011, **44**, 1018-1028.
8 T. Riley, T. Govender, S. Stolnik, C. D. Xiong, M. C. Garnett, L. Illum and S. S. Davis, *Colloids Surf. B*, 1999, **16**, 147-159.
9 N. R. Jana, *Phys. Chem. Chem. Phys.*, 2011, **13**, 385-396.
10 F.-L. Mi, Y.-C. Tan, H.-F. Liang and H.-W. Sung, *Biomaterials*, 2002, **23**, 181-191.
11 I. Bala, S. Hariharan and M. N. Kumar, *Crit. Rev. Ther. Drug Carrier Syst.*, 2004, **21**, 387-422.
12 H. S. Choi, W. Liu, P. Misra, E. Tanaka, J. P. Zimmer, B. I. Ipe, M. G. Bawendi and J. V. Frangioni, *Nat. Biotechnol.*, 2007, **25**, 1165-1170.
13 O. C. Farokhzad and R. Langer, *ACS Nano*, 2009, **3**, 16-20.
14 M. N. V. R. Kumar, R. A. A. Muzzarelli, C. Muzzarelli, H. Sashiwa and A. J. Domb, *Chem. Rev.*, 2004, **104**, 6017-6084.
15 J. Panyam and V. Labhasetwar, *Adv. Drug Delivery Rev.*, 2003, **55**, 329-347.
16 R. A. Jain, *Biomaterials*, 2000, **21**, 2475-2490.
17 J. Cheng, B. A. Teply, I. Sherifi, J. Sung, G. Luther, F. X. Gu, E. Levy-Nissenbaum, A. F. Radovic-Moreno, R. Langer and O. C. Farokhzad, *Biomaterials*, 2007, **28**, 869-876.
18 H. Sun, B. Guo, X. Li, R. Cheng, F. Meng, H. Liu and Z. Zhong, *Biomacromolecules*, 2010, **11**, 848-854.
19 K. Prompruk, T. Govender, S. Zhang, C. D. Xiong and S. Stolnik, *Int. J. Pharm.*, 2005, **297**, 242-253.
20 H.-M. Yang, C. W. Park, S. Lim, S.-I. Park, B. H. Chung and J.-D. Kim, *Chem. Commun.*, 2011, **47**, 12518-12520.
21 N. R. Jana, N. Erathodiyil, J. Jiang and J. Y. Ying, *Langmuir*, 2010, **26**, 6503-6507.
22 S. Han, Y. Liu, X. Nie, Q. Xu, F. Jiao, W. Li, Y. Zhao, Y. Wu and C. Chen, *Small*, 2012, **8**, 1596-1606.
23 W. Lin and D. Kim, *Langmuir*, 2011, **27**, 12090-12097.
24 H. Chen, L. Xiao, Y. Anraku, P. Mi, X. Liu, H. Cabral, A. Inoue, T. Nomoto, A. Kishimura, N. Nishiyama and K. Kataoka, *J. Am. Chem. Soc.*, 2014, **136**, 157-163.
25 M.-H. Lai, S. Lee, C. E. Smith, K. Kim and H. Kong, *ACS Appl. Mater. Interfaces*, 2014, **6**, 10821-10829.
26 H. Lee, S. M. Dellatore, W. M. Miller and P. B. Messersmith, *Science*, 2007, **318**, 426-430.
27 E. Amstad, T. Gillich, I. Bilecka, M. Textor and E. Reimhult, *Nano Lett.*, 2009, **9**, 4042-4048.
28 W. Wang, X. Ji, H. B. Na, M. Safi, A. Smith, G. Palui, J. M. Perez and H. Mattoussi, *Langmuir*, 2014, **30**, 6197-6208.
29 M. E. Lynge, R. van der Westen, A. Postma and B. Städler, *Nanoscale*, 2011, **3**, 4916-4928.
30 C. Missale, S. R. Nash, S. W. Robinson, M. Jaber and M. G. Cargon, *Physiol. Rev.*, 1998, **78**, 189-225.
31 P. Sokoloff, B. Giros, M.-P. Martres, M.-L. Bouthenet and J.-C. Schwartz, *Nature*, 1990, **347**, 146-151.
32 J. L. Scemama, C. Ruellan, P. Clerc, F. Clemente and A. Ribet, *Int. J. Cancer*, 1984, **34**, 675-679.
33 S. J. Clarke, C. A. Hollmann, Z. Zhang, D. Suffern, S. E. Bradforth, N. Dimitrijevic, W. G. Minarik and J. L. Nadeau, *Nat. Mater.*, 2006, **5**, 409-417.
34 S. J. Clarke, C. A. Hollmann, F. A. Aldaye and J. L. Nadeau, *Bioconjugate Chem.*, 2008, **19**, 562-568.
35 M. Tomida, T. Nakato, S. Matsunami and T. Kakuchi, *Polymer*, 1997, **38**, 4733-4736.
36 M. C. A. Stuart, J. C. van de Pas and J. B. F. N. Engberts, *J. Phys. Org. Chem.*, 2005, **18**, 929-934.
37 H. Ceylan, M. Urel, T. S. Erkal, A. B. Tekinay, A. Dana and M. O. Guler, *Adv. Funct. Mater.*, 2013, **23**, 2081-2090.
38 M. Cencer, Y. Liu, A. Winter, M. Murley, Hao. Meng and B. P. Lee, *Biomacromolecules*, 2014, **15**, 2861-2869.

39 S. Mandal, C. Banerjee, S. Ghosh, J. Kuchlyan and N. Sarkar, *J. Phys. Chem. B*, 2013, **117**, 6957-6968.

40 F.-Q. Hu, L.-N. Liu, Y.-Z. Du and H. Yuan, *Biomaterials*, 2009, **30**, 6955-6963.

41 E. A. Simone, T. D. Dziubla and V. R. Muzykantov, *Expert Opin. Drug Delivery*, 2008, **5**, 1283-1300.

42 D. D. Lasic, *Nature*, 1996, **380**, 561-562.

43 M. Saad, O. B. Garbuzenko, E. Ber, P. Chandna, J. J. Khandare, V. P. Pozharov and T. Minko, *J. Controlled Release*, 2008, **130**, 107-114.

44 P. J. Photos, L. Bacakova, B. Discher, F. S. Bates and D. E. Discher, *J. Controlled Release*, 2003, **90**, 323-334.

45 S. Muro, C. Garnacho, J. A. Champion, J. Leferovich, C. Gajewski, E. H. Schuchman, S. Mitragotri and V. R. Muzykantov, *Mol. Ther.*, 2008, **16**, 1450-1458.

46 Y. Geng, P. Dalhaimer, S. Cai, R. Tsai, M. Tewari, T. Minko and D. E. Discher, *Nat. Nanotechnol.*, 2007, **2**, 249-255.

47 S. Cai, K. Vijayan, D. Cheng, E. M. Lima and D. E. Discher, *Pharm. Res.*, 2007, **24**, 2099-2109.

48 L. Rajendran, H.-J. Knölker and K. Simons, *Nat. Rev. Drug Discovery*, 2010, **9**, 29-42.

49 J. Zhao, J. Liu, S. Xu, J. Zhou, S. Han, L. Deng, J. Zhang, J. Liu, A. Meng and A. Dong, *ACS Appl. Mater. Interfaces*, 2013, **5**, 13216-13226.

50 G. S. R. Raju, E. Pavitra, G. P. Nagaraju, K. Ramesh, B. F. El-Rayes and J. S. Yu, *Dalton Trans.*, 2014, **43**, 3330-3338.

51 B. Khorsand, G. Lapointe, C. Brett and J. K. Oh, *Biomacromolecules*, 2013, **14**, 2103-2111.

52 C. A. Reddy, V. Somepalli, T. Golakoti, A. K. R. Kanugula, S. Karnewar, K. Rajendiran, N. Vasagiri, S. Prabhakar, P. Kuppusamy, S. Kotamraju and V. K. Kutala, *PLoS One*, 2014, **9**, e89351.

53 G. R. Chamberlain, D. V. Tulumello and S. O. Kelley, *ACS Chem. Biol.*, 2013, **8**, 1389-1395.

Dopamine functionalized, polyaspartamide-based polymeric nanoparticle has been synthesized for selective delivery of drugs to human colon adenocarcinoma cells.